Carbonate chemistry in sediment pore waters of the Rhône River delta driven by early diagenesis (NW Mediterranean)

Jens Rassmann[1], Bruno Lansard[1], Lara Pozzato[1,2], Christophe Rabouille[1]

[1]Laboratoire des Sciences du Climat et de l'Environnement, LSCE/IPSL, CEA-CNRS-UVSQ-Université Paris Saclay, Gif-sur-Yvette, 91198, France

[2]Institut Méditerranéen d'Océanologie, CNRS-IRD-Université de Toulon-Aix Marseille, 13288 France

Corresponding author: Jens Rassmann (jens.rassmann@lsce.ipsl.fr)

Abstract. The Rhône River is the largest source of terrestrial organic and inorganic carbon for the Mediterranean Sea. A large fraction of this terrestrial carbon is either buried or mineralized in the sediments close to the river mouth. This mineralization follows aerobic and anaerobic pathways with a range of impacts on calcium carbonate precipitation and dissolution in the sediment near the sediment-water interface. This study focusses on the production of dissolved inorganic carbon (DIC) and total alkalinity (TA) by early diagenesis, consequential pH variations and the effect on calcium carbonate precipitation or dissolution. The sediment pore water chemistry was investigated along a transect from the Rhône River outlet to the continental shelf. Concentrations of DIC, TA, SO_4^{2-} and Ca^{2+} were analyzed on bottom waters and extracted sediment pore waters, whereas pH and oxygen concentrations were measured *in situ* using microelectrodes. The average oxygen penetration depth into the sediment was 1.7 ± 0.4 mm close to the river mouth and 8.2 ± 2.6 mm in the continental shelf sediments, indicating intense aerobic respiration rates. Diffusive oxygen fluxes through the sediment-water interface ranged between 3 and 13 mmol O_2 m^{-2} d^{-1}. In the first 30 cm of the sediment, DIC and TA pore water concentrations increased with depth up to 48 mmol L^{-1} near the river outlet and up to 7 mmol L^{-1} on the shelf as a result of aerobic and anaerobic mineralization processes. Due to oxic processes, at all stations pH decreased by 0.6 pH units in the oxic layer of the sediment accompanied by a decrease of the saturation state regarding calcium carbonate. In the anoxic layer of the sediments, sulfate reduction was the dominant mineralization process and was associated to an increase of pore water saturation state regarding calcium carbonate. Ultimately anoxic mineralization of organic matter caused calcium carbonate precipitation demonstrated by a large decrease in Ca^{2+} concentration with depth in the sediment. Carbonate precipitation decreased in the offshore direction, together with the carbon turnover and sulfate consumption in the sediments. The large production of pore water alkalinity characterizes these sediments as an alkalinity source to the water column which may increase the CO_2 buffering capacity of these coastal waters. Estuarine sediments should therefore receive more attention in future estimations of global carbon fluxes.

1 Introduction

The coastal ocean is a net sink of atmospheric CO_2 and plays an important role in the global carbon cycle (Hedges and Keil, 1995; Chen and Borgès, 2009; Bauer et al., 2013; Laruelle et al., 2013). This dynamic region is not only a sink for atmospheric CO_2, but also a location where terrestrial organic and inorganic carbon is buried or recycled (Hedges and Keil, 1995; Cai, 2011). Due to strong pelagic-benthic coupling, a large fraction of organic matter (OM) is mineralized in continental shelf sediments (McKee et al., 2004; Burdige, 2011; Bauer et al., 2013). Estuaries and deltas are a very dynamic part of coastal ocean regions, characterized by high carbon turnover (Hedges and Keil, 1995; Cai, 2011). They are the principal link between continents and oceans and receive inputs of terrestrial organic and inorganic carbon, in both, particulate and dissolved phases (McKee et al., 2004; Cai, 2011; Dai et al., 2012; Bauer et al., 2013). An important fraction of these inputs remains on site and undergoes oxic and anoxic mineralization (Andersson et al., 2005; Aller and Blair, 2006; Chen et al., 2012). Despite their importance for the coastal carbon cycle, there is a lack of knowledge about the links between early diagenesis and the carbonate system in river dominated sediments (McKee et al., 2004).

Aerobic and anaerobic reaction pathways contribute to the production of dissolved inorganic carbon (DIC) resulting in the acidification of the bottom waters. Anaerobic reactions also lead to production of total alkalinity (TA) that increases the CO_2 buffer capacity of seawater (Thomas et al., 2009). Variations in DIC and TA affect the partial pressure of CO_2 (pCO_2) in seawater and ultimately the CO_2 exchange with the atmosphere (Emerson and Hedges, 2008). By increasing the CO_2 buffer capacity of seawater, the release of TA from anaerobic sediments into the water column could account for a majority of the CO_2 uptake in shelf regions and deliver as much TA to the oceans as is derived from rivers (Thomas et al., 2009). Due to high dynamics, spatial heterogeneity and complex biogeochemical mechanisms, estimations of TA fluxes from the sediments are affected by high uncertainties (Krummins et al., 2013). The processes by which TA is produced in the sediments are still not well understood. Anaerobic respiration (e.g. denitrification, sulfate reduction, iron and manganese reduction) may play a major role, although dissolution/precipitation of calcium carbonate may also have a large impact on TA concentrations (Jahnke et al., 1997; Thomas et al., 2009, Krumins et al., 2013). Indeed, the changes in sediment pore water composition and pH can lead to over or under saturation of the calcium carbonate saturation state (Ω), and therefore influence carbonate dissolution and burial in sediments. Furthermore, carbonate dissolution was correlated to alkalinity fluxes across the sediment-water interface (SWI) (Mucci et al., 2000).

Using *in situ* microelectrode measurements, Komada et al. (1998) and Cai et al. (2000) investigated small scale changes in pCO_2, pH and DIC in deep marine sediments and the exchange fluxes associated. In continental shelf sediments, Mucci et al. (2000) found that oxic mineralization can induce carbonate

dissolution below the sediment-water interface, extending the observations of Jahnke et al., (1997, 2004) to coastal sediments. Burdige et al., (2008, 2010) pointed out that carbonate dissolution is also driven by oxic respiration in the shallow carbonated sediments of the Bahamas Bank. Concerning anoxic processes, Van Capellen and Wang (1996) demonstrated that high manganese and iron contents in the sediments of the Skagerrak (Eastern North Sea) and associated OM mineralization can increase pore water pH by proton-consuming reduction processes of oxidized iron and manganese. These authors highlighted the complexity of the multiple competing reaction pathways in anoxic sediments and observed that the existing theoretical background (e.g. Froelich et al., 1979, Berner, 1980) was insufficient.

In regions with a high carbon turnover, sulfate reduction is a large contributor to anoxic early diagenesis and can even be the dominant mineralization process for OM (Mucci et al., 2000; Burdige and Komada, 2011; Pastor et al., 2011). Sulfate reduction slightly decreases pH (Jourabchi et al, 2005; Soetaert et al., 2007), but nevertheless, it tends to enhance carbonate precipitation because of its coupling with precipitation of sulfide minerals from iron oxides (Gaillard et al., 1989; Mucci et al., 2000; Burdige, 2011). As an example, in sapropelic sediments from a Mangrove Lake, Mackenzie et al. (1995) reported a stable pH throughout the sulfate-reduction zone and a buildup of supersaturation with respect to carbonate with depth. These results contrast with the theoretical perspective that sulfate reduction was supposed to lead to carbonate dissolution because of the pH decrease (Jourabchi et al., 2005). Even today, the reproduction of measured pore water profiles in the sediments and the estimation of TA and DIC fluxes across the SWI by modeling are very challenging (Arndt et al., 2013; Krumins et al., 2013; Jourabchi et al., 2005). In addition, the magnitude of DIC and TA fluxes across the SWI are not well constrained and can vary significantly between different study sites (Mucci et al., 2000).

The objective of this study is to improve our understanding of the influence of early diagenesis of organic matter on carbonate dissolution and precipitation, and the production of DIC and TA. Therefore, we collected seawater and sediment samples along a transect from the Rhône River delta to the Mediterranean Sea continental shelf covering a broad range of biogeochemical characteristics (Lansard et al., 2008; Cathalot et al., 2010; Cathalot et al. 2013). The Rhône River delta receives inputs of terrestrial organic and inorganic carbon, in both particulate and dissolved phases which decrease with the distance to the river mouth. The majority of these inputs remains on site and undergo mineralization in the sediments (Pastor et al., 2011a). Therefore sediments display strong spatial gradients in biogeochemical parameters such as nutrients, organic and inorganic carbon, affecting the diagenetic transport-reaction network (Bourgeois et al., 2011; Lansard et al., 2009). High sedimentation rates and resuspension events make this environment very dynamic and heterogeneous (Cathalot et al., 2010). The "predominance" of sediment accumulation over other dynamic processes and the absence of tidal mixing and dominant marine currents differentiate the prodelta of the Rhône differs from other deltaic

environments like the Amazon, where the surface sediments are constantly reworked (Aller et al., 1998). Previous studies in this region often focused on organic matter mineralization pathways measurements in the oxic sediment layers and analysis of particulate carbon (Lansard et al., 2008; Cathalot et al., 2010) or could not provide simultaneous DIC and TA pore water measurements (Pastor et al., 2011a). These studies did not provide information on TA production and fluxes at the SWI. Accordingly, we designed a study to investigate the interaction of mineralization processes on pore water pH and the fate of solid calcium carbonates. For that purpose, we used a combination of i*n situ* oxygen and pH microelectrode measurements and pore water analysis of DIC, TA, SO_4^{2-} and Ca^{2+} concentrations to examine various diagenetic pathways on different vertical scales. We investigated a transect of stations characterized by various biogeochemical conditions (from oxic-dominated to sulfate reduction-dominated sediments). Furthermore, we calculated and discussed the calcium carbonate saturation state in regards to the different intensity of biogeochemical processes in these river-dominated sediments and estimated how early diagenesis impacts the bottom water carbonate chemistry (DIC, TA and pCO_2).

2 Study site and methods

2.1 The Rhône River delta

With a drainage basin of 97 800 km^2 and a mean water-discharge of 1700 $m^3\ s^{-1}$, the Rhône River is the largest river of the Mediterranean Sea in terms of fresh water discharge, inputs of sediment and terrestrial organic and inorganic matter (Pont, 1997; Durrieu de Madron et al., 2000; Sempéré et al., 2000). The Rhône River mouth is a wave-dominated delta located in the microtidal Mediterranean environment of the Gulf of Lions (Sempéré et al., 2000). Its river plume is mostly oriented southwestward, due to the Coriolis Effect and the wind forcing (Estournel et al., 1997). The annual discharge of particulate inorganic carbon (PIC) is estimated to be $0.68 \pm 0.45\ 10^9$ gC yr^{-1} (Sempéré et al., 2009). The total particulate organic carbon (POC) deposition in the Rhône delta system (265 km^2) is approximately $100 \pm 31\ 10^9$ gC yr^{-1} with the deltaic front accounting for nearly 60 % of the total POC deposition (Lansard et al., 2009). In front of the river mouth, the deposited sediments are of a cohesive nature and composed of fine grained sediments (e.g. > 90 % silt and clay) (Roussiez et al., 2005; Lansard et al., 2007). Previous studies demonstrated that the carbonate content in the surface sediments varies between 28 and 38 % (Roussiez et al., 2006) and the content of organic carbon (OC) varies between 1 and 2 % (Roussiez et al., 2005, 2006; Lansard et al., 2008, 2009). The PIC in the sediments is composed by autochtonous and allochtonous carbonates with the most abundant calcifying organisms in this area being foraminifera (Mojtahid et al., 2010).

The seafloor bathymetry shows that the delta is divided in three zones, characterized by different water depth, sedimentation rate and strength of continental slope. Got and Aloisi (1990) defined three major

domains: the Proximal domain, in a radius of 2 km from the river outlet with water depth ranging from 10 to 30 m, the Prodelta domain, between 2 and 5 km from the river mouth with depth ranging from 30 to 70 m, and the Distal domain, with depth between 70 and 80 m passed the 5 km from the river mouth. Annual sedimentation rates reach up to 30-48 cm yr^{-1} close to the river mouth (Charmasson et al., 1998) and rapidly decrease below 0.1 cm yr^{-1} on the continental shelf (Miralles et al., 2005). The seafloor in this region is a dynamic environment driven by sediment accumulation and with important heterogeneity regarding diagenetic activities, sediment pore water profiles and exchange fluxes at the sediment-water interface (Lansard et al., 2009; Cathalot et al., 2010). Diffusive oxygen fluxes into the sediment show spatial variability, both with the distance from the river mouth (decreasing in offshore direction) and on the horizontal scale of a few cm^2 (Lansard et al., 2009; Pastor et al., 2011b). Anoxic mineralization processes play a major role in the Prodelta sediments and are dominated by iron and sulfur cycling (Pastor et al., 2011a).

2.2 Sampling Stations

Ten stations have been sampled along the main direction of the Rhône River plume during the DICASE oceanographic cruise that took place in the Gulf of Lions between June 2-11, 2014 on board of the RV Tethys II (http://dx.doi.org/10.17600/14007100). The positions and main characteristics of the sampling stations are shown in Figure 1 and in Table 1. The stations were between 2 and 25 km distance from the Rhône River mouth, covering a bathymetric gradient ranging from 20 m to 80 m of water depth and representing the three different domains (A, Z : Proximal Domain; AK, B, K, L : Prodelta Domain and C, D, E, F : Distal Domain). The stations in the proximal domain A and Z have been sampled twice, in order to investigate spatial variability at these two stations. During this cruise, a benthic lander was used to measure *in situ* oxygen and pH micro profiles and sediment cores were taken for pore water extraction and solid phase analysis. The cruise took place during a period of low water discharge (957 $m^3\ s^{-1}$) and air temperatures between 20 °C and 30 °C.

2.3 *In situ* measurements

To measure *in situ* oxygen and pH micro profiles at the sediment-water interface, an autonomous lander (Unisense®) was used. This lander is equipped with a high precision motor capable of simultaneously moving five oxygen microelectrodes (Revsbech, 1989), two pH microelectrodes and a resistivity probe (Andrews and Bennet, 1981) with a vertical resolution of 100 µm. The recorded oxygen profiles were calibrated using oxygen concentrations measured in bottom waters (BW) by Winkler Titration (Grasshoff et al., 1983) and the zero oxygen measured in the anoxic zone (Cai and Sayles, 1996). The SWI was positioned where the strongest vertical oxygen gradient was measured (Rabouille et al., 2003). The calibration of the pH electrodes was carried out using NBS buffers, thus allowing the estimation of the slope of the electrode signal in function of pH variation at onboard temperature. The slope was then

recalculated at *in situ* temperature and the electrode signal variation was transformed into pH changes. The pH of bottom waters was determined using the spectrophotometric method with m-cresol purple following Clayton and Byrne, (1993) and Dickson et al., (2007). Pore water pH on the total proton scale (pH_t) was recalculated using the signal of the microelectrode adjusted to this pH-BW value. At each depth, the profiler waited for 20 s to stabilize the electrode before measurements were recorded. Each data point is an average of five measurements carried out at every depth. For all *in situ* profiles, the signal drift of each microelectrode was examined to ensure it was < 5 % from the beginning to the end of the measurements. The slope of the pH electrodes was double checked to make sure it was at least 95 % of the theoretical slope from the Nernst equation of -59 mV per pH-unit at 25 °C. At each station, 5 oxygen profiles and two pH profiles were measured simultaneously on a sediment surface of 109 cm^2.

2.4 Calculation of oxygen fluxes across the sediment-water interface

Sediment oxygen uptake rate has been widely used to assess benthic OC mineralization during early diagenesis. The total oxygen uptake (TOU) rate can be split into two parts: (i) the diffusive oxygen uptake rate (DOU), and (ii) the advective oxygen uptake. The DOU rates were calculated using Fick's first law (Berner, 1980):

$$DOU = -D_s \cdot \varphi \frac{d[O_2]}{dz}|z=0 \quad (1)$$

with:

D_s : apparent diffusion coefficient adjusted for diffusion in porous environment calculated following

$D_s = \frac{D_0}{1+3\cdot(1-\varphi)}$ where D_0 is the diffusion coefficient in free water according to (Broecker and Peng, 1974)

ϕ : sediment porosity

$\frac{d[O_2]}{dz}|z=0$: Oxygen gradient at the sediment-water interface

2.5 Sampling and *ex situ* measurements

Bottom water samples were collected with a12-L Niskin bottle as close as possible to the seafloor at each station. For these samples, temperature was measured using a digital thermometer with a precision of 0.1 °C and salinity was measured with a salinometer having a precision of 0.1. The pH, concentrations of DIC, TA and dissolved O_2 were measured on board within one hour for pH and within

six hours for DIC and TA. The pH of seawater was measured using a spectrophotometer and m-cresol purple as dye (Clayton and Byrne, 1993; Dickson et al., 2007) with uncertainties smaller than 0.01 pH units. Oxygen concentrations were determined using Winkler titration with an average uncertainty of 0.4 µmol L^{-1}. All DIC concentrations (bottom waters and pore waters) were measured on a DIC analyzer (Apollo SciTech®) using 1 ml sample volume with 4 to 6 replicates. The principle of the method is to acidify the sample with 10 % phosphoric acid to transform all forms of DIC into CO_2. The sample is then outgassed using ultra-pure nitrogen as a vector gas. The degassed CO_2 is quantified by a LICOR® gas analyzer, containing a non-dispersive infrared detector (NDIR). To calibrate the method, a certified reference material (CRM-batch #122, provided by A. Dickson, Scripps Institution of Oceanography) was used at least twice a day to confirm the accuracy of the DIC and TA measurements. TA concentrations were measured in a potentiometric open cell titration on 3 ml sample volume (Dickson et al., 2007). In our study, TA refers to total alkalinity, including silicates, phosphates, sulfides, organic alkalinity, etc.. The DIC and TA uncertainties in the sediment pore waters were below 0.5 %.

Sediment cores were sampled using an UWITEC® single corer (60 cm length, 9.5 cm inner diameter). After sampling, the cores were rapidly introduced in a glove bag with a N_2 atmosphere, to avoid oxidation, and pore waters were extracted using Rhizons, with pore size of 0.1-0.2 µm (Seeberg-Elverfeldt et al., 2005). The Rhizons had been degassed and stored in a N_2-filled gas tight box before use. Pore waters were extracted with a 2 cm vertical resolution and split into subsamples for DIC, TA, SO_4^{2-} and Ca^{2+} analysis. Sulfate concentrations were measured in the laboratory using a turbidimetric method (Tabatai, 1974). Concentrations of calcium ions were measured using ICP-AES (Ultima 2, Horiba®) by the "Pôle Spectométrie Océan" in Brest (France) with a relative uncertainty of 0.75 %. The calcium concentrations were salinity corrected by assuming constant Na^+ concentrations with depth in the pore water to avoid any evaporation effects due to sample storage. All bottom water concentrations were measured as triplicates. Small sample volumes in pore waters only allowed for replicates for the DIC, SO_4^{2-} and Ca^{2+} analysis but not for TA.

At each station, additional cores were taken for solid phase analysis. To establish porosity profiles, fresh sediment samples were weighed, dried for one week at 60 °C and weighed again. Knowing the salinity and density of seawater and sediment, porosity was calculated from the weight loss after drying. Total carbonate content of the solid phase was analyzed using a manocalcimeter with uncertainties of 2.5 % of $CaCO_3$. A manocalcimeter is a small, gastight container where the sediment can be acidified with HCl to dissolve calcium carbonates. The resulting increase of pressure is measured with a manometer and is directly proportional to the carbonate content of the sediment sample. Sediment samples have also been analyzed to quantify the calcite/aragonite proportion via X-Ray diffraction (XRD) on a X-Pert Pro diffractometer, using the θ-θ technique with the K-α-line of copper. The uncertainties of the XRD measurements were below 5 % of the aragonite proportion (Nouet and Bassinot, 2007).

2.6 Calculation of carbonate speciation, $CaCO_3$ saturation states and pH in pore waters

According to Orr et al. (2015), the best way to compute the 9 parameters of the carbonate system at *in situ* conditions is to start with DIC and TA concentrations. The thermodynamic constants proposed by Lueker et al. (2000) were used to calculate DIC speciation and pore water pH with the program CO2SYS (Lewis and Wallace, 1998). The calcium carbonate saturation state, for both calcite and aragonite, is expressed as the solubility product of calcium and carbonate ions concentrations divided by their solubility constant k_{sp} :

$$\Omega_{Ca} = \frac{\left[Ca^{2+}\right]\left[CO_3^{2-}\right]}{k_{sp}} \quad (2)$$

The solubility constant k_{sp} was calculated for *in situ* temperature, salinity and pressure following Millero et al. (1979), Mucci (1983) and Millero (1995).

3 Results

3.1 Bottom waters

In June 2014, the Rhône River water discharge was low and close to 1000 $m^3\ s^{-1}$ for the previous 2 months. Accordingly, the extent and thickness of the Rhône River plume were limited and bottom waters were not influenced by the river outflow, even close to the river mouth. Bottom water temperature, salinity, O_2, DIC, TA, pH, SO_4^{2-} and pCO_2, are reported in Table 1. Salinity remained very constant close to the seafloor, whereas temperature decreased with water depth from 16.8 to 14.3°C. Bottom waters were well oxygenated and oxygen concentrations decreased also with increasing water depth. DIC and TA concentrations varied slightly and the TA/DIC ratio in the bottom waters of all stations was 1.1 ± 0.02. The pH of bottom water was locally variable with a general decrease in offshore direction. SO_4^{2-} concentrations were constant between the stations with typical values for seawater around 30 mmol L^{-1}. During the sampling period, the Integrated Carbon Observation System (ICOS) station at Manosque (l'Observatoire de Haute Provence, https://icos-atc.lsce.ipsl.fr/?q=OHP) measured a pCO_2 of 410 ppm. At most stations, the bottom water pCO_2 was oversaturated compared to the atmosphere, with the lowest values calculated close to the river mouth (stations A and Z) and the highest values calculated at the shelf stations

3.2 The oxic layer

Figure 2 shows all oxygen profiles measured *in situ* during the DICASE cruise. The oxygen penetration depth (OPD) into the sediment was 1.7 ± 0.4 mm in the proximal domain, 3.3 ± 1.3 mm in the prodelta domain and 8.2 ± 2.6 mm in the distal domain. Some profiles had burrows creating small oxygen peaks below the OPD. The diffusive oxygen uptake rate (DOU) calculated from the measured oxygen profiles are plotted in Figure 3 as a function of the distance to the river mouth in the direction of the river plume. The positive value signifies an uptake of O_2 into the sediment. The DOU decreases exponentially with distance from 12.3 ± 1.1 mmol m^{-2} d^{-1} at station A towards the minimum flux of 3.8 ± 0.9 mmol m^{-2} d^{-1} at station F.

In situ pH micro profiles were measured in the top 4 cm of the sediment at all stations (Fig. 4). Immediately below the SWI, the pH decreases by 0.6 to 0.7 pH units in the oxic layer. Similarly to the oxygen micro profiles, the pH gradient in the OPD is stronger close to the river mouth and weaker in the distal domain. Just below the first drop, pH increases by 0.1-0.2 pH units and tends towards an asymptotic value between 7.4 to 7.6. The pH inflexion point, i.e. where the pH decrease stops and pH starts increasing, is located deeper in the distal zone than in the proximal zone, just below the OPD. Note that pH profiles show high spatial heterogeneity, even at one station.

3.3 DIC and TA pore water concentrations and calculated pH

Figure 5 shows the DIC and TA pore water profiles measured during the DICASE cruise. All pore water gradients across the sediment-water interface were strongest close to the river mouth and decreased in offshore direction. At the SWI, the DIC gradients were stronger than the TA gradients for all stations. Despite the spatial heterogeneity in the sediments, the three major areas defined by Got and Aloisi 1990) in this region display different biogeochemical gradients. Accordingly, stations from each group will be reported and discussed separately. In the proximal domain (stations A and Z), DIC and TA concentrations increase immediately below the SWI and reach a maximum value of 48 mmol L^{-1} at 20 cm depth in the sediments, where the concentrations stabilize. In the prodelta domain (stations AK, B, K and L), DIC and TA concentrations increase to values of 5 mmol L^{-1} in the first 10 to 15 cm depth. Below this depth, the gradients become stronger and TA and DIC concentrations increase up to 12 to 15 mmol L^{-1} at the bottom of the cores (i.e. around 25 cm). This succession of two different gradient shapes in the TA and DIC profile is also observed in the distal domain (stations C, D, E and F), but the absolute values of the gradients are weaker. In the first 10 to 15 cm, the concentrations reach values of 3.5 mmol L^{-1} and increase up to 5 to 7.5 mmol L^{-1} at the bottom of the core. These very high DIC concentrations in the sediment are related to large DIC and TA gradients which are 4 to 10 times stronger in the proximal domain than at the other sites. The DIC and TA pore water profiles are well correlated in each core and the concentrations show a linear correlation with a slope of 1.01 and an $r^2 = 0.998$ (130 data points).

The sediment pH profiles were calculated from TA and DIC concentrations using CO2SYS. The pH is reported on the total proton scale (pH_T). In the first mm, the pH drops at all stations due to aerobic respiration (Figure 6). Below the oxygen penetration depth, the pH varies between 7.2 and 7.8 and converges towards the range of 7.4 to 7.6.

Existing numerical tools are developed for the water column, although we used them in the sediments knowing that pore water concentrations (e.g. DIC, TA,) are much larger than those in the water column. Despite this potential artifact, the calculated outputs (e.g. pH) agree with our measurements. A linear relationship of the pH data measured with microelectrodes against calculated pH by CO2SYS shows a correlation with a slope of 1.01 +/- 0.02 and an $r^2 = 0.7483$ (graph not shown).

3.4 Calcium and sulfate concentrations

At all stations, bottom water Ca^{2+}concentration varies between 10 and 11 mmol L^{-1} (Fig. 7). In the proximal domain, the Ca^{2+} concentration decreases just below the SWI to reach a minimum of 2 mmol L^{-1} at 15-20 cm depth, where DIC and TA concentrations reach a maximum and sulfate concentration a minimum. In the prodelta domain, the Ca^{2+} concentration remains stable with depth until 10-15 cm in relation to the weaker TA and DIC gradients (Fig. 7). Below this depth, where the TA and DIC gradients increase, Ca^{2+} decreases to values around 7 mmol L^{-1} at the bottom of the cores. The distal domain is characterized by constant Ca^{2+} concentrations which remain above 10 mmol L^{-1}.

In extracted sediment pore water, sulfate concentrations range from 5 to 32 mmol L^{-1} from the surface down to 30 cm depth. Our measurements indicate strong sulfate consumption rates in the proximal domain (Fig. 8) where DIC and TA gradients are strong as well. In the proximal domain, sulfate concentration decreases in the first cm below the SWI compared to the bottom water. In the prodelta domain, sulfate reduction starts to occur between 10 and 15 cm depth, the same depth where TA and DIC gradients increase. In the distal domain, no significant sulfate reduction occurs in the first 30 cm, as sulfate concentration remains constant and TA and DIC gradients are low compared to the other domains.

3.5 Solid carbonates and calcium carbonate saturation state

The carbonate content of the solid phase scattered around 35 % at all stations, from the surface down to 30 cm. The composition of sedimentary $CaCO_3$ was dominated by calcite (≈ 95 %), with a small fraction of magnesian calcite (< 5 %), and only traces of aragonite (data not shown). Accordingly, only $\Omega_{calcite}$ is reported since calcite is dominant and aragonite is insignificant in the sedimentary $CaCO_3$. The $CaCO_3$ saturation state, calculated with CO2SYS from our TA/DIC and Ca^{2+} data, is presented on figure 9 for the three domaines. At all stations, the calcite saturation state in pore waters drops in the oxic layer. In the proximal domain (Fig. 9), the saturation state increases immediately below this first drop to

reach very high values of around 5 to 10. In the prodelta domain, the saturation state remains very close to 1 at a depth between 5 and 10 cm before increasing to super saturation (3 to 4) below 10 to 15 cm depth. In the distal domain, the saturation state shows no variation below the first drop into the sediment.

4 Discussion

4.1 Principal diagenetic reactions and their influence on the carbonate system

As the diagenetic transport-reaction network is complex, so are the interactions of these reactions with carbonate chemistry (Krumins et al., 2013). Table 2 summarizes the main diagenetic reactions (simplified) and their impact on DIC and TA pore water concentrations. DIC is always produced by OM mineralization and decreases pH, whereas the TA budget of these reactions and the resulting pH variation can be positive or negative. The dissolution and dissociation of metabolic (or atmospheric) CO_2 in seawater results in the formation of carbonic acid (R1), the consumption of CO_3^{2-} and ultimately leads to carbonate dissolution (R2a). Aerobic mineralization consumes O_2 and produces CO_2, decreasing pH without TA production (R3) and finally decreases Ω. In the sediments, oxygen is also used to reoxidise reduced species, a process that decreases pH even more strongly than aerobic respiration (R4-6) and thus reoxidation decreases Ω as well. In contrast, anaerobic mineralization causes much weaker pH reductions compared to the oxic processes and can even increase pH (R7-10). OM mineralization by nitrate reduction produces DIC and TA, has been related to TA release from the sediments and is even estimated to be a major TA source to the oceans. Sulfate reduction is usually associated with a weak decrease in pH, although with significant DIC and TA production. The resulting sulfide ions can either diffuse towards the surface to be oxidized within the oxic layer or precipitate with iron. The precipitation of sulfur minerals does not affect the amount of pore water DIC, but can have major influence on pH and TA (R11-13). The two reactions R14 and R15 deal with the coupling of sulfate reduction and methanogenesis and its impact on DIC.

In the Rhône River delta sediments, OM mineralization leads to DIC production, and under anoxic conditions, also to TA production. Our results demonstrate strong DIC and TA pore water gradients in the anoxic layer of the sediments indicating high anaerobic respiration rates. As a result, DIC and TA diffuse towards the SWI. No reaction in the oxic zone consumes DIC except potential carbonate precipitation. Our results indicate that more DIC is produced in the sediments than consumed by precipitation of $CaCO_3$. This means, that OM mineralization in the sediments leads to strong DIC fluxes from the sediments into the water column. For TA, the situation is more complicated, as oxidation of reduced species can consume as much TA as has been produced to reduce these species (Table 2). In a 1D system, where no precipitation occurs and no reduced species can be exported, 100 % of the anaerobic TA would be consumed in the oxic layer.

Krumins et al., (2013) reported that the effective TA flux from the sediments into the water column is far less important than the anaerobic TA production due to the TA loss in the oxic layer. Unfortunately, the resolution of the DIC and TA pore water profiles in this current study does not give precise information about the gradients in the oxic layer. Thus, we can only speculate about the oxic TA consumption in this region and related TA fluxes across the SWI. According to Pastor et al. (2011a), 97 % of the reduced species precipitate in the anoxic sediments in the Rhône prodelta. Therefore, the majority of the produced TA is likely released into the water column which can counterbalance the effects of the DIC fluxes and increase the CO_2 buffer capacity of the overlaying waters.

4.2 The impact of oxic and suboxic processes on the carbonate system

The upper part of the sediment, is defined as the oxic zone, supporting aerobic respiration (R3 – Table 2). Generally, the oxygen penetration depth (OPD) is related to aerobic respiration rates (Cai and Sayles, 1996). Aerobic respiration consumes O_2 to mineralize organic matter, produces metabolic CO_2 in the sediment pore water, increases the DIC concentration, lowers pH and possibly decreases the $CaCO_3$ saturation state (Cai et al., 1993, 1995). The OPD and oxygen fluxes are therefore key parameters to assess the effect of aerobic respiration on calcium carbonate in the sediment (Jahnke et al., 1997; Jahnke and Jahnke, 2004).

In the Rhône River delta, the OPD increases with water depth and distance from the Rhône River mouth as reported in previous studies (Lansard et al., 2008, 2009; Cathalot et al., 2010). These low values of O_2 penetration depths are classical for river-dominated ocean margins and they depend mainly on the sedimentation rate, the OM flux, the age and the oxidation state of OM (Lansard et al., 2009, Cathalot et al. 2013). Few *in situ* O_2 profiles show oxygen peaks at depth below the OPD. These are likely the effect of sediment bioturbation by the benthic macrofauna. As reported by Bonifácio et al. (2014), the macrofauna community is dominated by polychaetes and the highest activity is found in the prodelta domain. Nevertheless, comparisons between TOU and DOU rates have demonstrated that DOU account for about 80 % of total oxygen uptake rate into the sediments (Lansard et al., 2008). As a consequence, diffusive transport is dominant compared to advective transport and bioturbation (i.e. bioirrigation and bioventilation). Diffusive O_2 fluxes calculated from *in situ* 1D micro profiles (Fig. 2) are therefore representative for total oxygen uptake rates. As shown in Fig. 3, the diffusive oxygen fluxes into the sediment decrease exponentially with the distance from the river mouth, from 12.3 ± 1.1 mmol O_2 m^{-2} d^{-1}, close to the Rhône River mouth, to 3.8 ± 0.9 mmol O_2 m^{-2} d^{-1} offshore. According to Pastor et al., (2011a), the POC flux in the proximal domain is one order of magnitude higher than in the offshore regions of the Rhône prodelta. This OM flux, especially its labile fraction, supports oxygen consumption and is completely mineralized in the oxic layer (Pastor et al., 2011a).

During aerobic respiration, the ratio of oxygen to DIC during OM mineralization is close to 1, according to the stoichiometry of reaction R3 (Table 2). As a result, DIC concentrations increase just below the SWI at all stations (Fig. 5). The balance between O_2 flux and carbon oxidation in the sediment is affected by O_2-consumption linked to the oxidation of inorganic species produced via anoxic OC degradation (NH_4^+, Fe^{2+}, Mn^{2+} and HS^-). The oxidation of reduced diagenetic products has a profound effect on pore water O_2 and pH profiles in O_2 limited sediments (Cai and Reimers, 1993). These reactions (R4 to R6), in addition to aerobic bacterial respiration, consume TA and decrease pore water pH and therefore decrease the calcium carbonate saturation state as well.

There is a large contribution of anoxic processes to total OM mineralization in sediments near the Rhône River mouth, certainly due to large inputs of fresh organic material combined with high sedimentation rates (Pastor et al., 2011a). The diagenetic by-products originally produced during anoxic mineralization are almost entirely precipitated and buried in the sediment, which leads to a relatively low contribution of the re-oxidation of reduced products to total oxygen consumption. Still, between 10 to 40 % of the oxygen flux is used to oxidize reduced species of iron and manganese, contributing to lower pH (Pastor et al., 2011a). Again, the upward flux of reduced species in the sediments is higher in the proximal domain than in the others. Offshore, less OM is available and the diagenetic activity is weaker, providing less reduced species from deeper sediment layers. The pH drops below the SWI, caused by all oxic processes, are visible on the *in situ* pH micro profiles and decreases until the OPD is reached (Figs. 2 and 4). As the OPD are smaller and the oxygen fluxes are higher in the proximal domain, the pH minimums are reached at shallower depth in the sediment than in the other domains. The pH drop is lowering Ω by consuming carbonate ions (Emerson and Hedges, 2008; Jourabchi et al., 2005). The decrease of Ω, due to both aerobic respiration and the oxidation of reduced species, is clearly visible between the first two points located above and below the SWI interface (Fig. 9).

In agreement with current understanding of anoxic diagenesis, the observed pH increase of 0.1 to 0.2 units below the OPD can be attributed to OM mineralization via reduction of iron and manganese (R8 and R9 – Table 2). These anoxic reactions release TA and increase pH in the oxic-anoxic transition zone (Aguilera et al., 2005; Jourabchi et al., 2005). This pH increase and the release of TA create a strong increase in the pore water saturation state (Ω). Previous researches indicated that the turnover of Fe and Mn is high in the sediments close to the river mouth (Pastor et al., 2011a). The first pore water data point sampled in the sediments represents a mixture of oxic and anoxic pore water. Therefore, we potentially over estimate Ω in the oxic layer based on calculations from pore water concentrations (Cai et al., 2010). Different measurements in the deep sea revealed that Ω shows a minimum in the oxic layer (Cai et al., 1993, 1995, 1996; Hales and Emerson, 1997). As pH decreased at all stations to the same value, but the TA and DIC gradients at the interface are the strongest in the proximal domain, Ω should show the highest values in the oxic sediments of the proximal domain and decrease in offshore

direction. High TA concentrations in the oxic layer resulting from anoxic OM mineralization below, prevent the carbonate saturation state from getting below 1. Thus, potential dissolution in the oxic layer would most likely occur in the distal domain, but could be inhibited in the proximal domain.

In contrast to other nearshore environments, nitrate reduction has been shown to account only for 2-5 % of OM mineralization in the sediments of the prodelta of the Rhône whereas other anaerobic mineralization processes account for 30-40 % in the distal domain and up to 90 % in the proximal domain (Pastor et al., 2011a). Nitrate reduction produces less TA than DIC (TA/DIC ratio = 0.8/1) and thus lowers Ω.

Finding this clear succession of reactions is interesting, particularly the pH profiles that look classical in the aerobic sediment layers sampled from this complex and dynamics system. As OPDs measure only a couple of mm, molecular diffusion is by far the dominant transport process (Peclet number $\gg 1$ on a scale of the OPD). The microstructure of these sediments is restored very fast after distrubances like resuspension events (Toussaint et al., 2014). Furthermore, the comparison with previous studies shows, that despite the high sediment dynamics in this region, the general biogeochemical tendencies are maintained throughout time.

4.3 Sulfate reduction and its impact on carbonate chemistry

With sulfate concentration in seawater around 30 mmol L^{-1}, SO_4^{2-} reduction can generate large amounts of DIC and TA during organic matter mineralization through sulfate reduction. Indeed, in organic rich sediments, sulfate reduction can account for the majority of OM mineralization (Gaillard et al., 1989; Jourabchi et al., 2005; Burdige, 2011; Fenschel et al., 2012). Following reaction R9, two units of DIC and TA are produced for one unit of sulfate consumed (Mucci et al., 2000; Krumins et al., 2013).

To estimate the actual $\Delta DIC/\Delta SO_4^{2-}$ ratio due to diagenetic processes, the slope of the correlation between produced DIC (ΔDIC) and consumed sulfates (ΔSO_4^{2-}) in the pore waters (Fig 10) has to be corrected for molecular diffusion following the equation proposed by Berner (1980). Accordingly, we used the diffusion coefficients determined by Li and Gregory (1973). Below 10 cm depth, the observed diffusion corrected $\Delta DIC/\Delta SO_4^{2-}$ ratio equals 1.8 ± 0.02. The deviation of this measured value, from the theoretical value of 2 can be linked to higher oxidation states of organic matter which increases the SO_4^{2-} requirement for DIC production (in an extreme case, if methane undergoes oxidation, the $\Delta DIC/\Delta SO_4^{2-}$ ratio equals 1), carbonate precipitation lowering DIC concentrations or methanogenesis that increases DIC without consuming SO_4^{2-} (Burdige and Komada, 2011; Antler et al., 2014). All three factors may interact in the proximal zone. A large OM fraction in this zone is of terrestrial origin, aged and partly oxidized before being deposited (Cathalot et al., 2013). Calcium carbonates precipitate in the

pore waters of these sediments (Fig. 7) and lower DIC concentrations. In addition, the presence of methane has been reported by Garcia-Garcia et al., (2006).

As demonstrated by Burdige (2011) and Burdige and Komada (2011), the interaction of all diagenetic pathways are hard to disentangle and do not provide clear evidence of changes in the $\Delta DIC/\Delta SO_4^{2-}$ ratio. Nonetheless, the value of the observed $\Delta DIC/\Delta SO_4^{2-}$ ratio (1.8 ± 0.1) points towards the dominance of sulfate reduction in the deeper layers of the sediment (below 10 cm depth). Despite all these diverse reactions that affect the $\Delta DIC/\Delta SO_4^{2-}$ ratio, they are balanced in a way that ΔDIC and ΔSO_4^{2-} correlate well and do not show a deviation in the slope throughout the whole sediment depth investigated (Figure 10).

Sulfate reduction is also attested by the co-production of alkalinity and DIC (Fig. 5) which is by far the most important alkalinity producer in marine sediments (Krumins et al., 2013). Sulfate reduction creates a TA/DIC ratio very close to 1 in the pore waters. This situation is very similar to Mangrove Lake sediments (Mackenzie et al., 1995) where depletion of sulphate is almost complete and DIC and TA concentrations build up to 40 mmol L^{-1} in the sediment pore waters, or to other coastal environments (Burdige, 2011; Antler et al., 2014). No other reaction in the anoxic zone has a TA/DIC production ratio near 1. As pH is buffered, probably by precipitation of FeS and FeS_2 (R12), this large increase of alkalinity is accompanied, in the proximal zone, by a large increase of the saturation state of pore waters with respect to calcite (Fig. 9) up to values of oversaturation (Ω) from 5 to 10.

The effect of sulphate reduction and the carbonate saturation state has been a matter of debate since the early work of Ben-Yaakov (1973). Indeed, sulphate reduction produces large quantities of both alkalinity, which increases Ω, and protons, which decrease Ω. This has been summarized in Jourabchi et al.'s model (2005) by estimating that sulphate reduction would lead to decrease of Ω if it was the only ongoing reaction. The sediments from the proximal area of the Rhône River delta show, on the contrary, that pH stabilizes between 7.2 and 7.6. In these sediments, mineralization is driven by sulphate reduction that generates an increase of saturation state with respect to calcite (Fig. 9). This situation is very similar to Mackenzie et al. (1995) and Mucci et al. (2000) who also showed an increase of Ω when sulphate reduction is significant. Using a closed system model, Ben Yaakov (1973) estimated that oxidation of HS^- coupled to iron hydroxide reduction with FeS precipitation (as in R11 or R12) would buffer or even increase pH.

The Rhône River is known to be the most important riverine input of iron into the Mediterranean Sea (Guieu et al., 1991) with an iron content varying between 2 and 4 % in the solid phase discharge. In the proximal zone of the Rhone Delta, dissolved sulphide is absent from the first tens of centimeters in the sediment (Pastor et al., 2011a) indicating that re-oxidation and/or precipitation of sulphide is occurring in these sediments. Pastor et al, (2011a) estimated that sulphides are the limiting factor for pyrite

precipitation in this environment. Therefore, Charles et al., (2014) suggested, that OM mineralization in the prodelta of the Rhône could be coupled to pyritisation. With this important FeS coupling, pH is stabilized or tends to increase and a large oversaturation with respect to calcium carbonate is created due to produced carbonate ions.

In the proximal domain, the large super saturation with respect to calcite, induces calcite precipitation as evidenced by a large decrease of dissolved calcium in the pore waters (Gaillard et al., 1989; Boudreau et al., 1992). Indeed, Ca^{2+} concentration decreases by 9 mmol L^{-1} between the bottom water and 25 cm depth in proximal sediments. This precipitation consumes about 10 to 15 % of anaerobically produced DIC and TA. Following R2b, this should affect the TA/DIC ratio, but the observations do not show any deviations of the TA/DIC ratio from 1. The missing TA is likely provided by pyrite formation (R12).

In the prodelta domain (Fig. 8), a similar set of reaction involving sulfate reduction and sulphide re-oxidation and precipitation is also visible with lower amplitude as sulfate depletion is only 5 mmol L^{-1}. Oversaturation with respect to calcite reaches values ranging from 3-4 only below 15 cm, and the Ca^{2+} decrease is limited and arises deeper. In the distal zone where Ω is around 2 down to 25 cm, no calcium decrease is visible indicating that precipitation does not occur.

As the alkalinity fluxes produced by anaerobic processes are high and likely not much reduced by reoxidation of reduced species in the oxic layer due to iron sulfide precipitation, net TA fluxes of the same order of magnitude than DIC fluxes are likely to occur. Therefore, the alkalinity build up in the anoxic zone could diffuse across the oxic sediment layer and contribute to buffer bottom waters and increase CO_2 storage capacity of these waters. The large precipitation of calcium carbonate in the proximal zone may have implications for the CO_2 source potential from the sediment. Indeed, calcium carbonate precipitation generates CO_2 (R2b) which can then be exported to the water column. In addition, calcium carbonate precipitation consumes TA. However, the order of magnitude of the TA consumption by carbonate precipitation in these sediments is below the quantity of TA produced by sulfate reduction. Without this TA flux, the pCO_2 of the bottom waters in the prodelta of the Rhône would likely be much higher than observed.

5 Conclusions

This study demonstrated that the three major domains of the Rhône River prodelta are characterized by different organic and inorganic particulate carbon interactions. Close to the river mouth, where the carbon turnover is highest, the biogeochemical gradients are the strongest, resulting in high chemical fluxes across the SWI. This confirms that the biogeochemistry in the prodelta region is driven by the import and processing of material from the Rhône River.

The oxic reactions produce CO_2 and create a pH drop of 0.6 to 0.8 pH units and reduce Ω. As a consequence, calcium carbonate might dissolve in the oxic layer, but the saturation state of bottom waters and pore waters just below the OPD suggest that this is unlikely to happen. The majority of oxygen is used for OM mineralization as most of reduced species precipitate in anoxic sediments and do not contribute to oxygen consumption. The mineralization of OM, presumably by Fe and Mn oxides, increases pH and Ω below the oxic layer to several mm in depth.

The strong TA and DIC gradients observed in the sediments of the Rhône River prodelta suggest that OM mineralization is dominated by anaerobic processes. Close to the river mouth, where the OC content in the sediments is highest, sulfate reduction is the dominant mineralization process for OM degradation creating a strong coupling between TA and DIC in pore water profiles. Despite its theoretical lowering effect on pH, sulfate reduction is related to an increase of Ω by important alkalinity production and via the simultaneous pH increase by precipitation of iron-sulfate-minerals. As a result, pore waters are over saturated at all sampled stations. Calcium carbonate precipitation occurs in the proximal and in the prodelta domain, depleting the majority of dissolved calcium ions in the proximal domain. This carbonate precipitation could represent an additional CO_2 source from the sediments to the water column, but is outbalanced by TA production by sulfate reduction. Due to this important anoxic TA production, the pCO_2 of bottom waters remain relatively low compared to the high release of DIC due to OM mineralization.

7 Acknowledgments

We thank David J. Burdige, an annonymous refereeand J. Patrick Laceby for their constructive comments that helped increase the quality of the paper. Furthermore, we would like to thank Bruno Bombed and Jean-Pascal Dumoulin for their technical help during the DICASE cruise and in the laboratory. We also thank the captain and crew of the RV Tethys II (INSU) for their excellent work at sea. A lot of our gratitude is for the SNAPO-CO2 for the inter-comparison of DIC and TA concentrations in our seawater samples. We are grateful to Celine Liorzou for the ICP-AES measurements, to Serge Miska for the help with the X-Ray diffraction analysis and we want to thank Stephanie-Duchamp-Alphonse to put a manocalcimeter at our disposition. This research was financed by the Mistrals / MERMEX project (http://mermex.pytheas.univ-amu.fr/?page_id=62) and through the MERMEX Rivers action.

References

Aguilera, D. R., Jourabchi, P., Spiteri, C. and Regnier, P.: A knowledge-based reactive transport approach for the simulation of biogeochemical dynamics in Earth systems: earth system dynamics, Geochem. Geophys. Geosy., 6, 1-18, 2005.

Aller, R. C.: Mobile deltaic and continental shelf muds as suboxic, fluidized bed reactors, Mar. Chem., 61, 143-155, 1998.

Aller, R. C. and Blair, N. E.: Carbon remineralization in the Amazon-Guianas tropical mobile mudbelt: A sedimentary incinerator, Cont. Shelf. Reas., 26, 2241-2259, 2006.

Andersson, A. J., Mackenzie, F. T., Lerman, A.: Coastal ocean and carbonate system in the high CO_2 world of the anthropocene, AM. J. Sci., 305, 875-918, 2005.

Andrews, D. and Bennet, A.: Measurements of diffusivity near the sediment-water interface with a fine-scale resistivity probe, Geochim. et Cosmochim. Acta, 45, 2169-2175, 1981.

Antler, G., Turchyn, A. V., Herut, B. Davies, A. and Rennie, V. C. F.: Sulfur and oxygen isotope tracing of sulfate driven anaerobic methane oxidation in estuarine sediments, Estuar. Coast. Shelf Sci., 142, 4-11, 2014.

Arndt, S., Jørgensen, B. B., LaRowe, D. E., Middleburg, J. J., Pancost, R. D. and Regnier, P.: Quantifiying the degradation of organic matter in marine sediments: A review and synthesis, Earth Sci. Rev., 123, 53-86, 2013.

Bauer, J. E., Cai, W.-J., Raymond, P. A., Bianchi, T. S., Hopkinson, C. S. and Regnier, P. A. G.: The changing carbon cycle of the coastal ocean, Nature, 504 (7478), 61–70, 2013.

Ben-Yaakov, S.: pH buffering of pore water of recent anoxic marine sediments, Limnol. Oceanogr., 18, 86–94, 1973.

Berner, R. A.: Early diagenesis: A theoretical approach, Princeton University Press, 241 pp., 1980.

Boudreau, B. P., Canfield, D. E. and Mucci, A.: Early diagenesis in a marine sapropel, Mangrove Lake, Bermuda, Limnol. and Oceanogr., 37, 8, 1738-1753, 1992.

Bourgeois, S., Pruski, A. M., Sun, M.-Y., Buscail, R., Lantoine, F., Vétion, G., Rivière, B. and Charles, F.: Distribution and lability of land-derived organic matter in the surface sediments of the Rhône prodelta and the adjacent shelf (Mediterranean sea, France): a multi proxy study, Biogeosciences, 8, 3107-3125, 2011.

Broecker, W. S. and Peng, T.-H.: Gas exchange rates between air and sea. Tellus, 26, 21–35, 1974.

Burdige, D. J., Zimmerman, R. C., and Hu, X.: Rates of carbonate dissolution in permeable sediments estimated from pore-water profiles: The role of sea grasses. Limnol. and Oceanogr., 53, 549-565, 2008.

Burdige, D. J., Hu, X. and Zimmermann, R. C.: The widespread occurence of coupled carbonate dissolution / reprecipitation in surface sediments on the Bahamas Bank, AM. J. Sci., 310, 492-521, 2010.

Burdige, D. J.: Estuarine and Coastal Sediments - Coupled Biogeochemical Cycling, Treatise Esturarine Coast. Sci., 5, 279–316, 2011.

Burdige, D. J. and Komada, T.: Anaerobic oxidation of methane and the stoichiometry of remineralization processes in continental margin sediments, Limnol. Oceanogr., 56(5), 1781–1796, 2011.

Cai, W. J., and Reimers, C. E.: The development of pH and pCO_2, microelectrodes for studying the carbonate chemistry of pore waters near the sediment-water interface, Limnol. and Oceanogr., 38, 1762-1773, 1993.

Cai, W. J., Reimers, C. E., and Shaw, T.: Microelectrode studies of organic carbon degradation and calcite dissolution at a California Continental rise site, Geochim. et Cosmochim. Acta, 59, 497-511, 1995.

Cai, W.-J., and Sayles, F. L.: Oxygen penetration depths and fluxes in marine sediments, Mar. Chem., 52, 123-131, 1996.

Cai, W.-J., Zhao, P. and Wang, Y.: pH and pCO_2 microelectrode measurements and the diffusive behaviour of carbon dioxide species in coastal marine sediments, Mar. Chem. 70, 133-148, 2000.

Cai, W.-J., Luther III, G. W., Cornwell, J. C. and Giblin, A. E.: Carbon Cycling and the Coupling Between Proton and Electron Transfer Reactions in Aquatic Sediments in Lake Champlain, Aquat. Geochem, 421-446, 2010.

Cai, W.-J.: Estuarine and Coastal Ocean Carbon Paradox: CO_2 Sinks or Sites of Terrestrial Carbon Incineration?, Annu. Rev. Mar. Sci., 3, 123–145, 2011.

Cathalot, C., Rabouille, C., Pastor, L., Deflandre, B., Viollier, E., Buscail, R., Grémare, A., Treignier, C. and Pruski, A.: Temporal variability of carbon recycling in coastal sediments influenced by rivers: assessing the impact of flood inputs in the Rhône River prodelta., Biogeosciences, 7, 1187-1205, 2010.

Cathalot, C., Rabouille, C., Tisnérat-Laborde, N., Toussaint, F., Kerhervé, P., Buscail, R., Loftis, K., Sun, M.-Y., Tronczynski, J., Azoury, S., Lansard, B., Treignier, C., Pastor, L. and Tesi, T.: The fate of river organic carbon in coastal areas: A study in the Rhône River delta using multiple isotopic (δ13C, Δ14C) and organic tracers, Geochim. Cosmochim. Acta, 118, 33–55, 2013.

Charles, F., Coston-Guarini, J., Lantoine, F., Guarini, J.-M. and Yücel, M.: Ecogeochemical fate of coarse organic particles in sediments of the Rhône River prodelta, Estuar. Coast. Shelf Sci., 141, 97–103, 2014.

Charmasson, S., Radakovitch, O., Arnaud, M., Bouisset, P. and Pruchon, A.-S.: Long-core profiles of ^{137}Cs, ^{134}Cs, ^{60}Co and ^{210}Pb in sediment near the Rhône River (Northwestern Mediterranean Sea), Estuaries, 21, 367–378, 1998.

Chen, C.-T. A. and Borges, A. V.: Reconciling opposing views on carbon cycling in the coastal ocean: Continental shelves as sinks and near-shore ecosystemsas sources of atmospheric CO_2 Deep-Sea Res. PT II, 56, 578–590, 2009.

Chen, C.-T. A., Huang, T.-H., Fu, Y.-H., Bai, Y. and He, X.: Strong sources of CO_2 in upper estuaries become sinks of CO_2 in large river plumes, Current Opinion in Environmental Sustainability, 4, 179-185, 2012.

Clayton, T. D. and Byrne, R. H.: Spectrophotometric seawater pH measurements: total hydrogen ion concentration scale calibration of m-cresol purple and at-sea results, Deep Sea Res. Part Oceanogr. Res. Pap., 40, 2115–2129, 1993.

Dai, M., Yin, Z., Meng, F., Liu, Q., Cai, W.-J.: Spatial distribution of riverine DOC inputs to the ocean: an updated global synthesis, Current Opinion in Encvironmental Sustainability, 4, 170-178, 2012.

Dickson, A.G., Sabine, C.L. and Christian, J.R.: Guide to best practices for ocean CO_2 measurements. PICES Special Publication 3, 2007.

Durrieu de Madron, X., Abassi, A., Heussner, S., Monaco, A., Aloisi, J. C., Radakovitch, O., Giresse, P., Buscail, R. and Kerherve, P.: Particulate matter and organic carbon budgets for the Gulf of Lions (NW Mediterranean), Oceanol. Acta, 23, 717–730, 2000.

Emerson, S. R. and Hedges, J. I.: Chemical Oceanography and the Marine Carbon Cycle, Cambridge University Press, 2008.

Estournel, C., Kondrachoff, V., Marsaleix, P. and Vehil, R.: The plume of the Rhone: numerical simulation and remote sensing, Cont. Shelf. Res., 17, 899-924, 1997.

Fenschel, T., King, G. M. and Blackburn, T. H.: Bacterial Biogeochemistry: The Ecophysiology of Mineral Cycling, 3rd ed., Academic Press (Elsevier)., 2012.

Froelich, P., Klinkhamm, G. P., Bender, M., Luedtke, N. A., Heath, G. R., Cullen, D., Dauphin, P., Hammond, D., Hartman, B. and Maynard, V.: Early oxidation of organic matter in pelagic sediments of the eastern equatorial Atlantic: suboxic diagenesis, Geochim. Cosmochim. Acta, 43, 1075–1090, 1979.

Gaillard, J.-F., Pauwels, H. and Michard, G.: Chemical diagenesis in coastal marine sediments, Oceanol. Acta, 12, 175-187, 1989.

García-García, A., Orange, D., Lorenson, T., Radakovitch, O., Tesi, T., Miserocchi, S., Berné, S., Friend, P. L., Nittrouer, C. and Normand, A.: Shallow gas off the Rhône prodelta, Gulf of Lions, Mar. Geol., 234, 215–231, 2006.

Got, H. and Aloisi, J. C.: The Holocene sedimentation on the Gulf of Lions margin: a quantitative approach, Cont. Shelf. Res., 10, 841-855, 1990.

Grasshoff, K. Ehrhardt, M, and K. Kremling.: Methods of Seawater Analysis. Grasshoff, Ehrhardt and Kremling, eds. Verlag Chemie GmbH. 419 pp., 1983.

Guieu, C., Martin, J. M., Thomas, A. J. and Elbaz-Poulichet, F.: Atmospheric Versus River Inputs of Metals to the Gulf of Lions, Total Concentrations, Partitioning and Fluxes, Mar. Poll. Bulletin, 22, 176-183, 1991.

Hales, B. and Emerson, S.: Calcite dissolution in sediments of the Cera Rise: In situ measurements of porewater O_2, pH and $CO_{2(aq)}$, Geochim. et Cosmochim. Acta, 61, 501-514, 1997.

Hedges, J. I. and Keil, R. G.: Sedimentary organic matter preservation: an assessment and speculative synthesis, Mar. Chem., 49, 81-115, 1995.

Jahnke, R. A., Craven, D. B., McCorkle, D. C., and Reimers, C. E.: $CaCO_3$ dissolution in California continental margin sediments: the influence of organic matter remineralization, Geochim. et Cosmochim. Acta, 61, 3587-3604, 1997.

Jahnke, R. A., and Jahnke, D. B.: Calcium carbonate dissolution in deep sea sediments: reconciling microelectrode, pore water and benthic flux chamber results, Geochim. et Cosmochim. Acta, 68, 47-59, 2004.

Jourabchi, P., Van Cappellen, P. and Regnier, P.: Quantitative interpretation of pH distributions in aquatic sediments: A reaction-transport modeling approach, Am. J. Sci., 305, 919–956, 2005.

Krumins, V., Gehlen, M., Arndt, S., Van Cappellen, P. and Regnier, P.: Dissolved inorganic carbon and alkalinity fluxes from coastal marine sediments: model estimates for different shelf environments and sensitivity to global change, Biogeosciences, 10, 371–398, 2013.

Lansard, B., Rabouille, C., Denis, L. and Grenz, C.: In situ oxygen uptake rates by coastal sediments under the influence of the Rhône River (NW Mediterranean Sea), Cont. Shelf Res., 28, 1501–1510, 2008.

Lansard, B., Rabouille, C., Denis, L. and Grenz, C.: Benthic remineralization at the land–ocean interface: A case study of the Rhône River (NW Mediterranean Sea), Estuar. Coast. Shelf Sci., 81, 544–554, 2009.

Laruelle, G. G., Dürr, H. H., Lauerwald, R., Hartmann, J., Slomp, C. P., Goossens, N. and Regnier, P. A. G.: Global multi-scale segmentation of continental and coastal waters from the watersheds to the continental margins, Hydrol. Earth Syst. Sci, 17, 2029-2051, 2013.

Lewis, E. and Wallace, D. W. R, Program developed for CO_2 system calculations. ORNL/CDIAC-105, Carbon Dioxide Information Analysis Center, US Department of Energy, Oak Ridge National Laboratory, Tennessee: http://cdiac.esd.ornl.gov/oceans/co2rprt.html, 1998.

Li, Y.-H. and S. Gregory: Diffusion of ions in sea water and in deep-sea sediments, Geochim. et Cosmochim. Acta, 88, 703-714, 1974.

Lueker, T. J., Dickson, A. G., Keeling, C. D.: Ocean pCO_2 calculated from dissolved inorganic carbon, alkalinity, and equations for K_1 and K_2 : validation based on laboratory measurements of CO_2 in gas and seawater at equilibrium, Mar. Chem., 70, 105-119, 2000.

Mackenzie, F. T. Vink, S., Wollast, R. and Chou, L.: Comparative Geochemistry of Marine Saline Lakes, Physics and Chemistry of Lakes, 2nd edition, Springer-Verlag, Berlin, 265-278, 1995

McKee, B.A., Aller, R.C., Allison, M.A., Bianchi, T.S. and Kineke, G.C.: Transport and transformation of dissolved and particulate materials on continental margins influenced by major rivers: benthic boundary layer and seabed processes, Cont. Shelf. Res.,24, 899-926, 2004.

Millero, F. J.: Thermodynamics of the carbon dioxide system in seawater, Geochim. Cosmochim. Acta, 43, 1651–1661, 1979.

Millero, F. J.: Thermodynamics of the carbon dioxide system in the oceans, Geochim. et Cosmochim. Acta, 59, 661-677, 1995.

Mojtahid, M., Jorissen, F., Lansard, B. and Fontanier, C.: Microhabitat selection of benthic foraminifera in sediments off the Rhône River mouth (NW Mediterranean), J. Foramin. Res., 40(3), 231–246, 2010.

Mucci, A.: The solubility of calcite and aragonite in seawater at various salinities, temperatures and one atmosphere total pressure, AM. J. Sci., 283, 780-799, 1983.

Mucci, A., Sundby, B., Gehlen, M., Arakaki, T., Zhong, S. and Silverberg, N.: The fate of carbon in continental shelf sediments of eastern Canada: a case study, Deep Sea Res. Part II Top. Stud. Oceanogr., 47, 733–760, 2000.

Nouet, J. and Bassinot, F.: Dissolution effects on the crystallography and Mg/Ca content of planktonic foraminifera *Gloorotalia tumida* (Rotaliina) revealed by X-ray diffractometry, Geochem. Geophy. Geosy., 8, Q10007, doi:10.1029, 2007.

Orr, J. C., Epitalon, J.-M. and Gattuso, J.-P.: Comparison of ten packages that compute ocean carbonate chemistry, Biogeosciences, 12, 1483–1510, 2015.

Pastor, L., Cathalot, C., Deflandre, B., Viollier, E., Soetaert, K., Meysmann, F.J.R., Ulses, C., Metzger, E. and Rabouille, C.: Modeling biogeochemical processes in sediments from the Rhône River prodelta area (NW Mediterranean Sea), Biogeosciences, 8, 1351-1366, 2011a.

Pastor, L., Deflandre, B., Viollier, E., Cathalot, C., Metzger, E., Rabouille, C., Escoubeyrou, K., Lloret, E., Pruski, A. M. and Vétion, G.: Influence of the organic matter composition on benthic oxygen demand in the Rhône River prodelta (NW Mediterranean Sea), Cont. Shelf Res., 31, 1008-1019, 2011b.

Pont D.: Les débits solides du Rhône à proximité de son embouchure : données récentes (1994-1995) / The discharge of suspended sediments near to the mouth of the Rhône recent statistics (1994-1995), Revue de géographie de Lyon, 72, 23-33, 1997.

Rabouille, C., Denis, L., Dedieu, K., Stora, G., Lansard, B. and Grenz, C.: Oxygen demand in coastal marine sediments: comparing in situ microelectrodes and laboratory core incubations, J. Exp. Mar. Biol. Ecol., 285, 49–69, 2003.

Revsbech, N. P.: An oxygen microsensor with a guard cathode, Limnol. and Oceanogr., 34, 474-478, 1989.

Roussiez, V., Aloisi, J.-C., Monaco, A. and Ludwig, W.: Early muddy deposits along the Gulf of Lions shoreline: A key for a better understanding of land-to-sea transfer of sediments and associated pollutant fluxes, Mar. Geol., 222-223, 345–358, 2005.

Roussiez, V., Ludwig, W., Monaco, A., Probst, J.-L., Bouloubassi, I., Buscail, R. and Saragoni, G.: Sources and sinks of sediment-bound contaminants in the Gulf of Lions (NW Mediterranean Sea): A multi-tracer approach, Cont. Shelf Reas. 26, 1843-1857, 2006.

Sempéré, R., Charrière, B., Van Wambeke, F. and Cauwet, G.: Carbon inputs of the Rhone River to the Mediterranean Sea: Biogeochemical implications, Glob. Biogeochem. Cycles, 14, 669-681, 2000.

Soetaert, K., Hofmann, A. F., Middleburg, J. J., Meysman, F. J. R. and Greenwood, J.: The effect of biogeochemical processes on pH, Mar. Chem., 105, 30-51, 2007.

Tabatai, M. A.: A rapid method for determination of sulfate in water samples, Environ. Lett., 7, 237–243, 1974.

Thomas, H., Schiettecatte, L.-S., Suykens, K., Koné, Y. J. M., Shadwick, E. H., Prowe, A. E. F., Bozec, Y., de Baar, H. J. W. and Borges, A. V.: Enhanced ocean carbon storage from anaerobic alkalinity generation in coastal sediments, Biogeosciences, 6, 267-274, 2009.

Toussaint F., Rabouille, C., Cathalot, C., Bombled, B., Abchiche, A., Aouji, O., Buchholtz, G., Clemençon, A., Geyskens, N., Répécaud, M., Pairaud, I., Verney, R. and Tisnérat-Laborde, N.: A new device to follow temporal variations of oxygen demand in deltaic sediments: the LSCE benthic station, Limnol. Oceanogr.: Methods, 12, 729-741, 2014

Van Cappellen, P. and Wang, Y.: Cycling of iron and Manganese in surface sediments: A general theory for the coupled transport and reaction of carbon, oxygen, nitrogen, sulfur, iron and manganese, AM J Sci., 296, 197-243, 1996.

Figure captions

Figure 1: Map of the Rhône River mouth (Northwestern Mediterranean Sea) with the stations investigated during the DICASE cruise in June 2014. The ocean bathymetry (in m) is indicated by the continuous lines.

Figure 2: All *in situ* oxygen micro profiles measured during the DICASE cruise, in the proximal, prodelta and distal domains. The sediment-water interface is marked by a horizontal line (depth = 0).

Figure 3: Diffusive oxygen uptake (DOU) across the sediment-water interface in function of the distance from the Rhône River mouth. The fluxes decrease exponentially following $DOU = F_{min} + Ae^{(-x/t)}$ with F_{min} being the flux in the offshore region, x the distance to the river mouth in km and, A and t being the numerical constants. Error bars are standard deviations between the diffusive fluxes calculated from the 5 single oxygen profiles measured at each station.

Figure 4: All pH_t micro profiles measured during the DICASE cruise in the proximal, prodelta and distal domains. The sediment-water interface is marked by a horizontal line.

Figure 5: DIC (black) and TA (red) pore water profiles in the first 40 cm of sediment in the proximal, the prodelta and the distal domains. For a better visibility of the profiles in each domain, the scale of the concentrations has been individually adjusted for each domain.

Figure 6: Calculated pH_t pore water profiles of the proximal, the prodelta and the distal domains. The error bars are estimations of the error propagation from the measured data in the calculation.

Figure 7: Pore water concentrations of Ca^{2+} (mmol L^{-1}); proximal domain in red, prodelta domain in blue and distal domain in black. The error bars represent the uncertainties of the ICP-AES measurements.

Figure 8 : Sulfate profiles measured in the pore waters (mmol L^{-1}) of the proximal, the prodelta and in the distal domains

Figure 9: Pore water calcium carbonate saturation state (Ω) of the proximal, prodelta and distal domain. The saturation limit for calcium carbonates dissolution/precipitation (Ω =1) is marked by a vertical line.

Figure 10: Scatter plot of ΔDIC vs ΔSO_4^{2-} with linear regression. Δ designates the difference between the corresponding pore water and bottom water concentration. The slope of the correlation is -1.65 +/- 0.017 with a correlation coefficient of $r^2 = 0.992$.

Figures

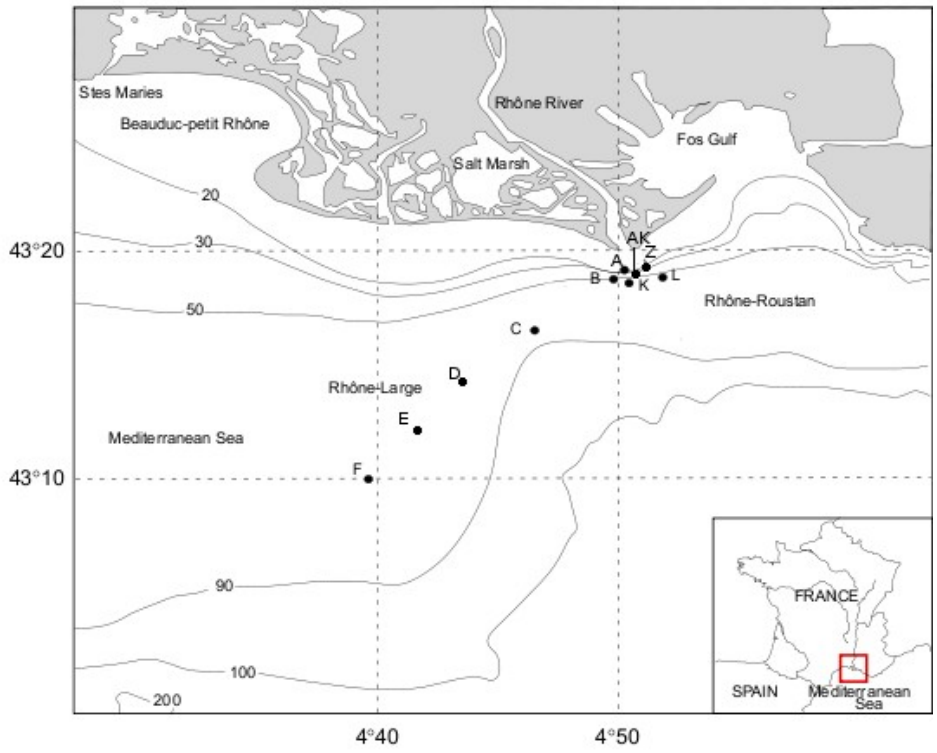

Figure 1

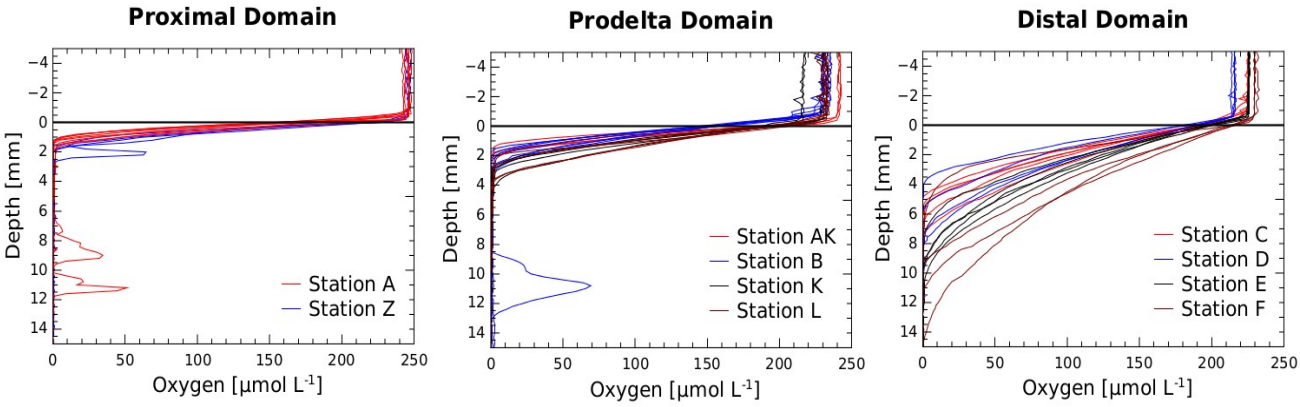

Figure 2

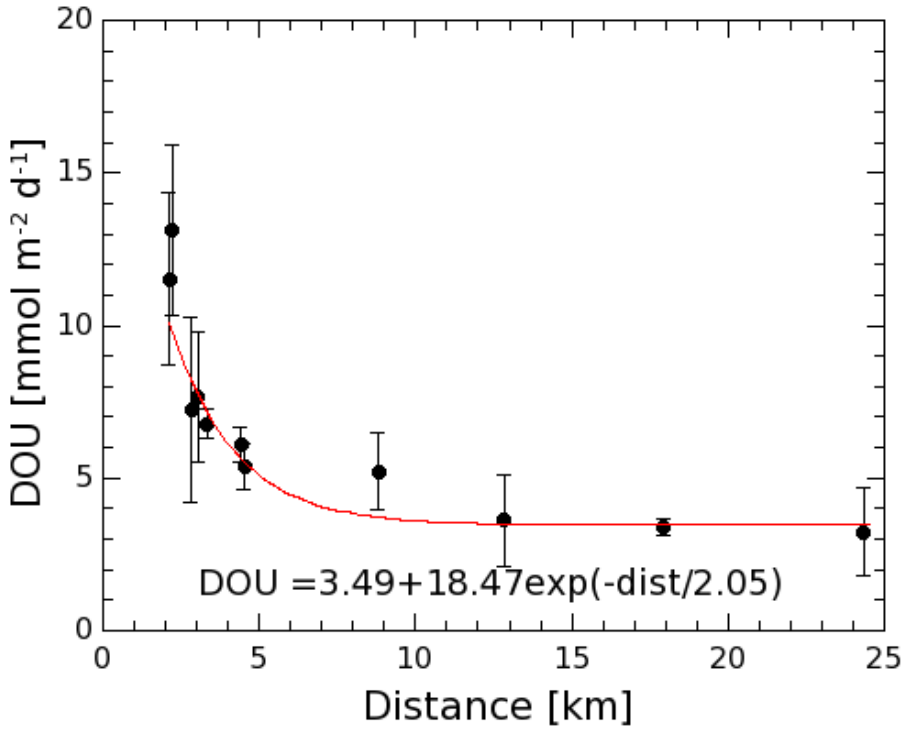

Figure 3

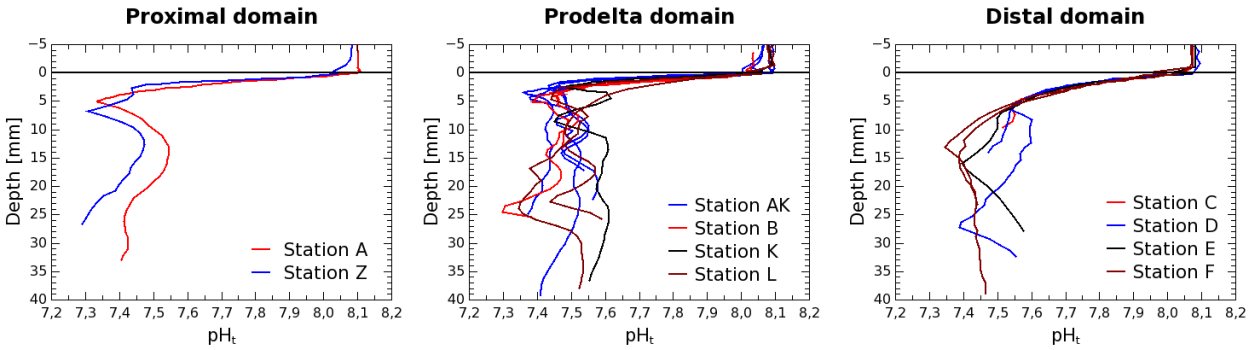

Figure 4

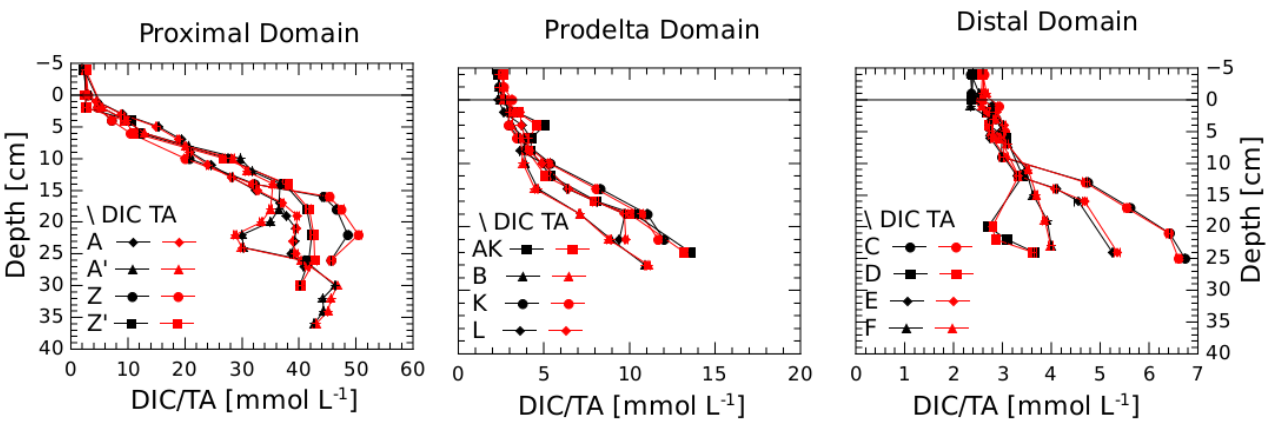

Figure 5

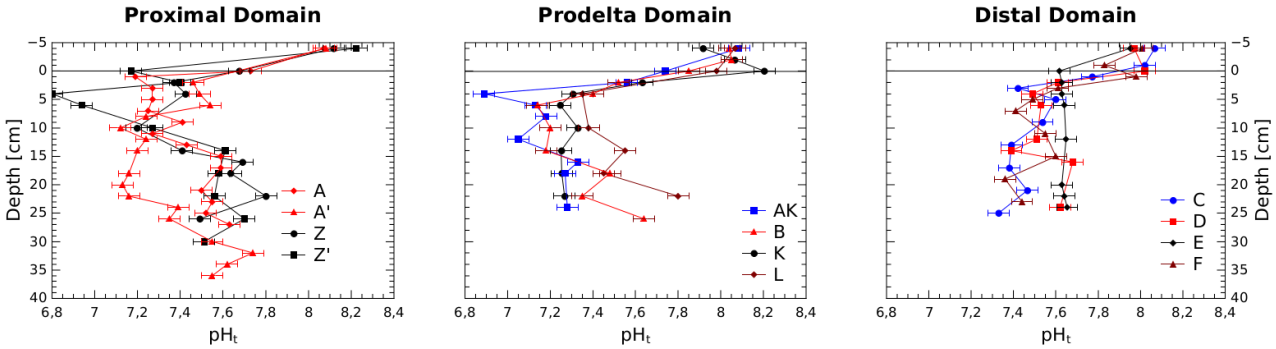

Figure 6

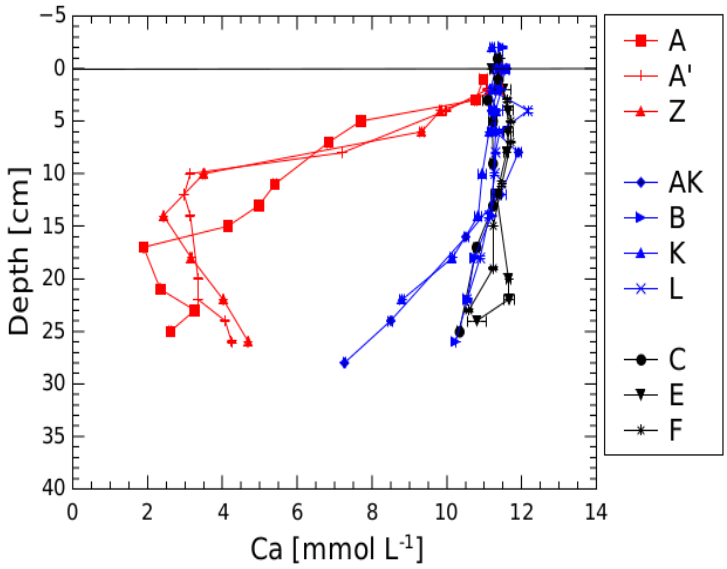

Figure 7

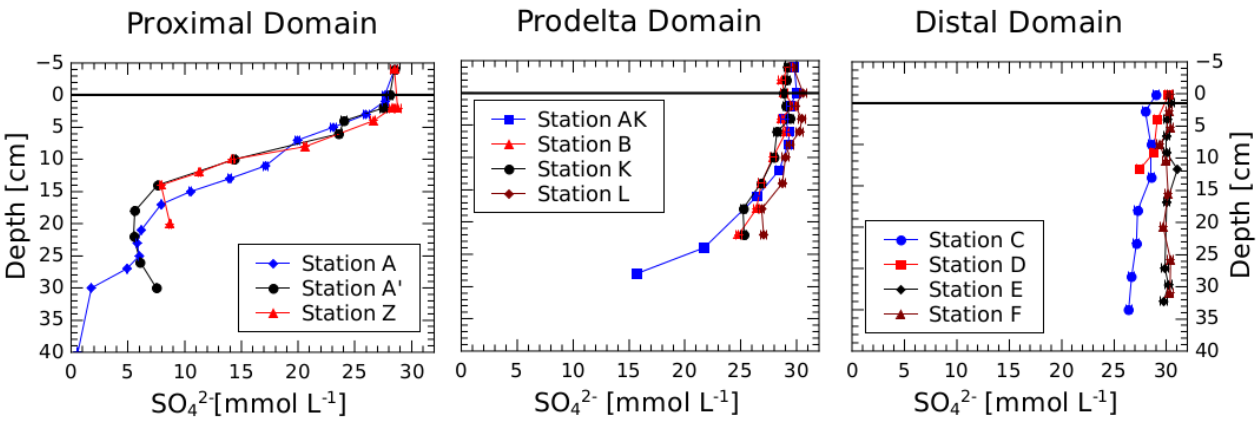

Figure 8

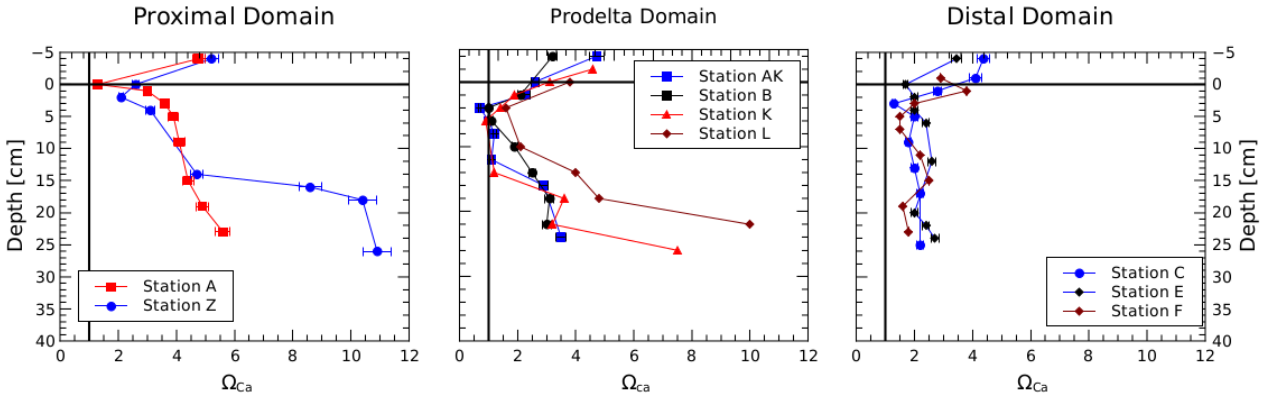

Figure 9

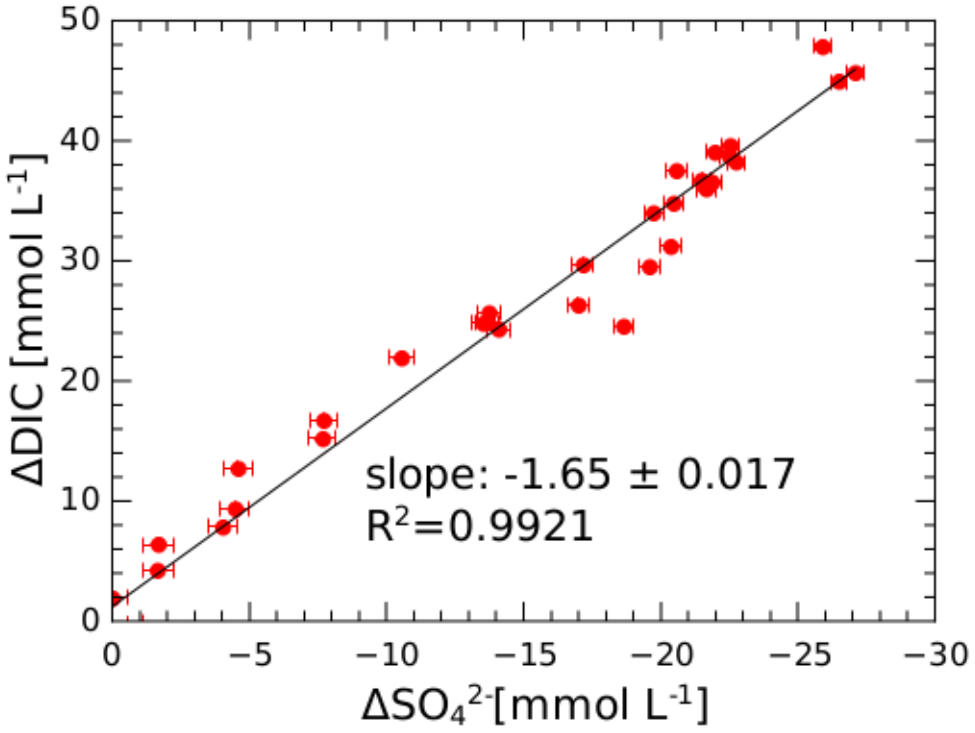
ΔDIC [mmol L-1]
ΔSO4 2- [mmol L-1]
slope: -1.65 ± 0.017
R2=0.9921
0
10
20
30
40
50
0
−5
−10
−15
−20
−25
−30

Figure 10

Tables

Table 1: Stations investigated during the DICASE cruise in June 2014 with the main properties of bottom waters; dist = distance from the Rhône river mouth

Station	Long. (°E)	Lat. (°N)	Dist. [km]	Depth [m]	T [°C]	Salinity	O_2 [µmol L^{-1}]	DIC [µmol L^{-1}]	TA [µmol L^{-1}]	pH_t	SO_4^{2-} [mmol L^{-1}]	pCO_2 (calculated) [µatm]
Z, Z'	4.865	43.317	2.2	18.0	16.0	37.5	244.0 ± 0.3	2330 ± 1	2648 ± 3	8.118 ± 0.003	28.4 ± 0.3	364.1
A, A'	4.851	43.312	2.1	18.3	16.8	37.7	245.1 ± 0.3	2323 ± 4	2613 ± 17	8.072 ± 0.004	28.2 ± 0.4	407.3
AK	4.856	43.307	2.8	48.1	15.8	37.4	240.8 ± 0.1	2335 ± 4	2623 ± 3	8.085 ± 0.011	29.7 ± 0.3	393.6
B	4.818	43.295	3.0	66.2	15.0	37.7	213.2 ± 0.8	2372 ± 5	2628 ± 2	8.039 ± 0.015	28.7 ± 0.3	446.1
K	4.856	43.302	3.3	60.5	14.9	37.7	226.4 ± 0.2	2351 ± 5	2538 ± 5	7.916 ± 0.002	29.1 ± 0.3	596.6
L	4.885	43.304	4.4	58.2	15.2	37.6	230.9 ± 0.6	2340 ± 2	2612 ± 5	8.066 ± 0.002	29.7 ± 0.3	412.4
C	4.773	43.271	8.8	75.0	14.4	37.7	225.6 ± 0.4	2354 ± 2	2621 ± 10	8.067 ± 0.004	29.0 ± 0.3	411.5
D	4.738	43.256	12.8	80.0	14.9	37.6	214.5 ± 0.5	2388 ± 8	2605 ± 3	7.970 ±	30.2 ± 0.3	531.3

									0.002		
E	4.685	43.219	17.9	77.3	14.3	37.7	226.3 ± 0.3	2391 ± 6	2594 ± 5	7.952 ± 0.004	30.4 ± 0.3	553.3
F	4.649	43.164	24.3	77.0	14.8	37.7	230.2 ± 0.1	2364 ± 4	2600 ± 24	8.008 ± 0.006	30.3 ± 0.3	478.4

705 Table 2: Diagenetic reactions and their effect on the carbonate system (TA, DIC, pH and Ω)

		Reaction	ΔTA/ΔDIC	ΔpH	Δ Ω
	Carbonate chemistry				
R1	CO_2 dissolution	$CO_2 + H_2O \leftrightarrow H_2CO_3 \leftrightarrow HCO_3^- + H^+ \leftrightarrow CO_3^{2-} + 2H^+$		-	-
R2a	Carbonate dissolution	$CaCO_3 + H_2O + CO_2 \rightarrow Ca^{2+} + 2HCO_3^-$	+ 2/1	+	+
R2b	Carbonate precipitation	$Ca^{2+} + 2\ HCO_3^- \rightarrow CaCO_3 + H_2O + CO_2$	-2/-1	-	-
	Aerobic reactions				
R3	Aerobic mineralization	$CH_2O + O_2 \rightarrow HCO_3^- + H^+$	0/1	-	-

R4	Nitrification	$NH_4^+ + 2O_2 \rightarrow NO_3^- + H_2O + 2H^+$	-2/0	-	-
R5	Iron oxidation	$4Fe^{2+} + O_2 + 10H_2O \rightarrow 4Fe(OH)_3 + 8H^+$	-8/0	-	-
R6	Manganese oxidation	$2Mn^{2+} + O_2 \rightarrow 2MnO_2$			
	Anaerobic Reactions				
R7	Nitrate reduction	$CH_2O + 0.8\,NO_3^- + 0.8\,H^+ \rightarrow CO_2 + 0.4\,N_2 + 1.4\,H_2O$	0.8/1	-	-
R8	Manganese reduction	$CH_2O + 2MnO_2 + 3H^+ \rightarrow HCO_3^- + 2Mn^{2+} + 2H_2O$	4/1	+	+
R9	Iron reduction	$CH_2O + 4Fe(OH)_3 + 7H^+ \rightarrow HCO_3^- + 4Fe^{2+} + 10H_2O$	8/1	+	+
R10	Sulfate reduction	$CH_2O + \frac{1}{2}SO_4^{2-} \rightarrow HCO_3^- + \frac{1}{2}HS^- + \frac{1}{2}H^+$	1/1	-	
R11	FeS precipitation	$Fe^{2+} + HS^- \rightarrow FeS + H^+$	-2/0	-	-
R12	FeS precipitation with sulfate recycling	$8Fe(OH)_3 + 9HS^- + 7H^+ \rightarrow 8FeS + SO_4^{2-} + 20H_2O$	-2/0	+	+
R14	Pyrite precipitation	$8Fe(OH)_3 + 15HS^- + SO_4^{2-} + 17H^+ \rightarrow 8FeS_2 + 28H_2O$	2/0	+	+
R15	Anaerobic methane oxidation	$CH_4 + SO_4^{2-} \rightarrow HS^- + HCO_3^- + H_2O$	2/1		+
R16	Methanogenesis	$CH_2O \rightarrow \frac{1}{2}CH_4 + \frac{1}{2}CO_2$	0/0.5	-	-